

Predicting the hydrolytic breakdown rates of organophosphorus chemical warfare agent simulants using association constants derived from hydrogen bonded complex formation events

Rebecca J. Ellaby, Dominique F. Chu, Antigoni Pépés, Ewan R. Clark & Jennifer Hiscock

To cite this article: Rebecca J. Ellaby, Dominique F. Chu, Antigoni Pépés, Ewan R. Clark & Jennifer Hiscock (2021) Predicting the hydrolytic breakdown rates of organophosphorus chemical warfare agent simulants using association constants derived from hydrogen bonded complex formation events, *Supramolecular Chemistry*, 33:6, 309-317, DOI: [10.1080/10610278.2021.1999450](https://doi.org/10.1080/10610278.2021.1999450)

To link to this article: <https://doi.org/10.1080/10610278.2021.1999450>



© 2021 The Author(s). Published by Informa UK Limited, trading as Taylor & Francis Group.



Published online: 10 Nov 2021.



Submit your article to this journal [↗](#)



Article views: 1566



View related articles [↗](#)



View Crossmark data [↗](#)



Citing articles: 4 View citing articles [↗](#)

Predicting the hydrolytic breakdown rates of organophosphorus chemical warfare agent simulants using association constants derived from hydrogen bonded complex formation events

Rebecca J. Ellaby^a, Dominique F. Chu^b, Antigoni Pépés^a, Ewan R. Clark^a and Jennifer Hiscock^a

^aSchool of Physical Sciences, University of Kent, Canterbury, Kent, UK; ^bSchool of Computing, University of Kent, Canterbury, Kent, UK

ABSTRACT

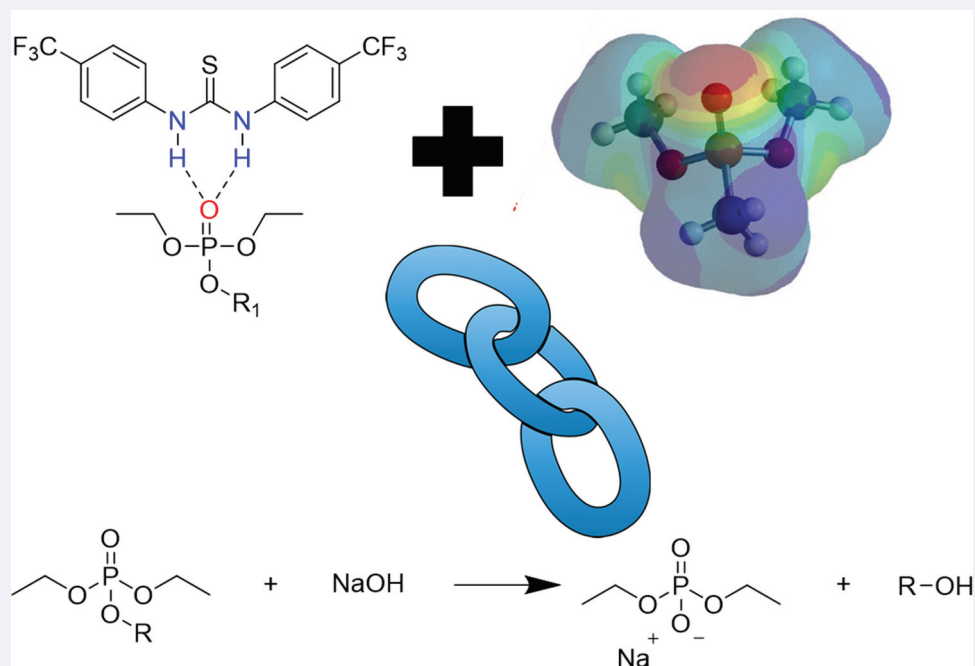
Organophosphorus (OP) chemical warfare agents (CWAs) represent an ongoing global threat, through either purposeful environmental release or the need to dispose of historic stockpiles. This presents a need for the development of novel decontamination technologies. Due to the toxic nature and legal limitations placed on OP CWAs, the use of appropriate OP simulants that mimic the reactivity but not the toxicity of the agents themselves is vital to decontamination studies. Herein, we show that association constants derived from non-specific hydrogen bonded complexation events may be used as parameters within models to predict simulant reactivity. We also discuss the limitations that should be placed on such data.

ARTICLE HISTORY

Received 29 July 2021
Accepted 21 October 2021

KEYWORDS

Hydrogen bond; simulant; chemical warfare agent; predictive models




Introduction

For almost a century, organophosphorus (OP) compounds have been used globally as pesticides and chemical warfare agents (CWAs)[1].[†] However, due to the inherent toxicity of these compounds combined with limited effective treatments [2,3], the accidental or purposeful release of these agents represents a continued global risk, as demonstrated by recent events in Germany (2020) [4], UK (2018) [5] and

Malaysia (2017) [6], as well as events in Syria (2013) [7] and Japan (1995)[8]. The ongoing development of novel decontamination and remediation technologies to limit the harmful effects of these OP compounds if released therefore remains imperative [2,9].

In general, OP simulants represent the only viable option when developing novel approaches both to combat OP CWA release and for subsequent remediation due to the highly toxic nature of, and legal restrictions

CONTACT Jennifer Hiscock  J.R.Hiscock@Kent.ac.uk  School of Physical Sciences, University of Kent, Canterbury, Kent

Provide short biographical notes on all contributors here if the journal requires them.

© 2021 The Author(s). Published by Informa UK Limited, trading as Taylor & Francis Group.

This is an Open Access article distributed under the terms of the Creative Commons Attribution License (<http://creativecommons.org/licenses/by/4.0/>), which permits unrestricted use, distribution, and reproduction in any medium, provided the original work is properly cited.

placed upon, the live agents themselves [10,11]. However, it is not feasible for any single simulant to simultaneously mimic all the chemical properties of an OP CWA without also inheriting undesirable molecular traits. Careful consideration of the appropriate properties of any simulant chosen to aid in the development of novel OP CWA detection, decontamination, or remediation methodologies [12–15] is therefore required.

Within the field of supramolecular chemistry, the use of CWA simulants to develop such technologies is well documented [16,17]. For example, Cragg and co-workers have highlighted the importance of simulant choice through their work comparing the coordination of OP CWAs and simulants binding within a cyclodextrin cavity [13–15]. These findings are further supported through the work of Barlaz and co-workers [12]. In addition, work by Gale and co-workers [18] have shown that simple tripodal compounds containing amino acids can not only bind to OP CWA agents but also enhance the rate of their hydrolysis. In further work, this research group also demonstrated the use of responsive supramolecular organogels for not only sensing the presence of OP CWAs but also CWA encapsulation and decontamination [19–21]. Furthermore, Ward and co-workers have demonstrated that supramolecular cages can be used for catalysing the hydrolysis of organophosphates upon binding within the cage cavity and on the cages exterior surface [22,23]. Similarly, Dennison and co-workers [24] have utilised a trivalent Europium complex to successfully bind a variety of OP structural analogues, to determine whether these could lead to the identification of next-generation VX simulants for supramolecular and spectroscopic purposes. Finally, work by Borguet, Rosi, Johnson and co-workers [25] has shown that DFT modelling can be used to predict ligand design for the uptake into metal-organic frameworks (MOFs) of the OP CWA simulant dimethyl methylphosphonate (DMMP).

Predictive models that utilise the derivation of potential simulant structure-desired physical property relationships (more generally referred to as structure activity relationships – SARs) can be used by researchers to aid the effective identification of appropriate OP CWA simulants. Specifically, they permit the screening of any potential target molecules without first requiring their synthesis, accelerating the development process [11,26,27], to identify the most appropriate simulant for the work to be undertaken. This approach, used by Snurr and Mendonca [28], drew upon density functional theory (DFT) studies on OP hydrolysis to develop a quantitative structure activity relationship (QSAR) model that supports the identification of appropriate OP CWA simulants for decontamination purposes.

Within our own work, we have demonstrated how simple, low-level computational modelling may be used to predict hydrogen bond mediated aggregation events [29,30], the resultant antimicrobial activity [31], and most recently to identify appropriate OP CWA simulants for the development of supramolecular detection technologies, through the calculation of association constants, which may be predicted using computationally derived parameters [11]. Herein, we build on this prior work, exploring the use of low-level computational modelling and supramolecular host:guest association constants to predict the reactivity of potential OP simulants towards the presence of NaOH, a base typically used within standard decontamination solutions [32,33], using a data set produced from the library of OP simulants **1–22**, [Figure 1](#). It is hoped that our preliminary work in this area will aid other researchers towards the identification of appropriate OP simulants for the development of novel decontamination technologies.

Synthesis

The synthesis of **1–23** ([Figure 1](#)) has been previously reported [11,34–42]. However, ¹H NMR spectra for these compounds have been provided within the supplementary information as evidence of sample purity.

Results and discussion

Assessing simulant reactivity

Several OP CWA decontamination solutions/systems are commercially available, these include the US army developed skin decontamination M258 kit [43], a two-phase system that contains two packets to be used sequentially. Packet 1 contains a towelette impregnated with phenol (10 wt %), ethanol (72 wt %), NaOH (5 wt %), ammonia (≈1 wt %), and water (12 wt %), whilst Packet 2 contains a towelette impregnated with chloramine-B and a sealed glass ampoule filled with zinc chloride [32,43]. DS2, a second decontamination solution, consists of diethylenetriamine (70 wt %), ethylene glycol monomethyl ether (28 wt %), and NaOH (2 wt %) [32,33]. Super tropical bleach (calcium hypochlorite (93 wt %) and NaOH (7 wt %)), when supplied as a solid or slurry with water is also considered useful for OP CWA decontamination [33,44]. With the partial exception of super-tropical bleach, all of these decontamination systems/solutions have in common the presence of an alcohol, NaOH, and H₂O. Here, the hydroxyl ion acts as a nucleophile, which attacks the electrophilic phosphorus centre, common to all members of this class

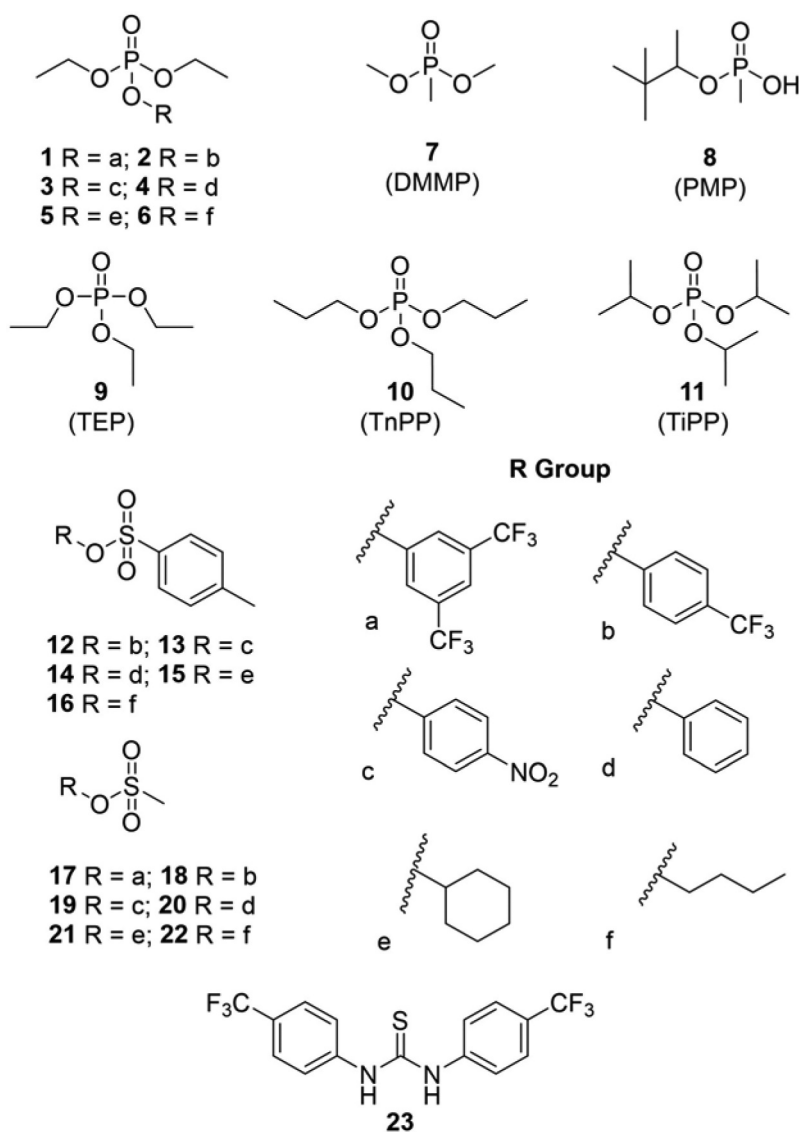
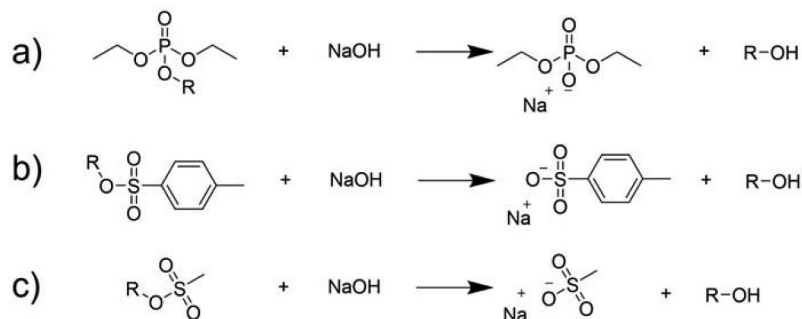


Figure 1. Chemical structures of compounds **1–23**.

of OP CWAs, neutralising/reducing the toxic effects of these agents [45–47]. When considering the library of potential simulants **1–22**, the electrophilic centre analogous to that of the OP CWA is either the analogous P = O phosphorus or O = S = O sulphur atom.

The reactivity of potential OP CWA simulants **1–22** was evaluated by reaction of these compounds (see [Scheme 1](#)) in the presence of five equivalents of NaOH, with respect to the simulant, at 291 K in a methanol- d_4 :D $_2$ O 70:30 solution. These experimental



Scheme 1. Reaction of OP simulants a) **1–11**, b) **12–16**, c) **17–22** with NaOH.

Table 1. Summary of average data ($n = 3$) obtained from the reaction of the appropriate OP CWA simulant **1–22** (10 mM) with 5 equivalence of NaOH (50 mM) in a methanol- d_4 :D₂O 70:30 solution at 291 K. Error = standard error of the mean.

OP CWA simulant	Simulant breakdown after 6 hours (%)	Rate order	Experimental rate constant (s^{-1})
1	92.8 (± 2.19)	1 st	0.42
2	47.9 (± 3.06)	1 st	0.22
3	100 ($\pm \leq 0.01$)	1 st	0.46
4	17.6 (± 0.01)	1 st	0.08
5	5.3 (± 0.23)	<i>a</i>	n/a
6	52.5 (± 0.01)	<i>a</i>	n/a
7	10.4 (± 0.01)	1 st	0.05
8	0 ($\pm \leq 0.01$)	-	-
9	0 ($\pm \leq 0.01$)	-	-
10	0 ($\pm \leq 0.01$)	-	-
11	0 ($\pm \leq 0.01$)	-	-
12	55.7 (± 2.24)	1 st	0.26
13	57.4 (± 0.06)	1 st	0.27
14	1.5 (± 0.05)	1 st	0.01
15	5.0 (± 0.36)	1 st	0.02
16	8.2 (± 0.52)	1 st	0.04
17	100 ($\pm \leq 0.01$)	<i>b</i>	-
18	80.9 (± 0.16)	2 nd	0.37 ^c
19	100 ($\pm \leq 0.01$)	<i>b</i>	-
20	2.1 (± 0.16)	<i>a</i>	n/a
21	66.5 (± 1.00)	1 st	0.31
22	94.1 (± 1.28)	1 st	0.44

a – Rate order could not be definitively assigned when fitting reaction data to either 1st order or 2nd order curves.

b – Rate of reaction could not be obtained due to speed of reaction being too fast to track using the NMR method.

c – Reaction rate units = $M^{-1} \cdot s^{-1}$.

conditions were a result of multiple optimisation studies in which [1]H NMR spectroscopy was used to monitor the relative proportions of reactant and simulant present with respect to time; the results of these studies have been summarised in Table 1. Due to the range of reaction rates observed for compounds **1–22** under these conditions, it was not possible to calculate experimental hydrolysis rate constants for all the simulants tested. Thus, the % simulant breakdown after 6 hours has been used as a comparative simulant reactivity value to create this dataset. This approach enabled us to include values generated from these studies for all the potential simulants. In addition, where an experimental rate constant could be calculated (**1–4**, **7**, **12–16**, **18**, **21–22**) all reactions were found to follow first order kinetics apart from that of compound **18** which was found to obey second order kinetics with respect to the simulant, at present the reason for this has not been determined. The specific reasons preventing rate order assignment are detailed within Table 1, and further supported by data supplied within the supplementary materials.[†]

Predicting simulant reactivity

A series of 1:1 host:guest association constants, determined by [1]H NMR in a CD₃CN solution at 298 K, have previously been reported for compounds **1–22** with **23**, a low molecular weight, non-specific, hydrogen bond donating receptor; these binding events have also been evaluated in terms of the series of computationally derived parameters listed in Table 2 [11]. We have previously reported the ability to use exhaustive parameter searches to rapidly identify predictive models for both the development of novel antimicrobials [31] and organophosphorus simulant binding [11]. Here, we used R data analysis software [48] to determine both direct and inverse predictive models for the percentage breakdown of potential chemical warfare agent simulants, building upon our previous work.

Organocatalysis by (thio)ureas is generally considered to arise from enhanced reactivity/electrophilicity of the substrate induced by hydrogen bonding with the catalyst, and catalyst efficacy is typically correlated with hydrogen bonding complexation strength of the substrate with the (thio)urea moiety [49–53]. We therefore hypothesised that 1:1 association constants, derived using a non-specific hydrogen bond donating receptor (**23**), could be used as a predictor of reaction centre electrophilicity when the principle hydrogen bond accepting group is directly joined to the reactive centre. Thus, we further hypothesise these association constants could be used in the prediction of reaction rates.

To test this hypothesis, we performed exhaustive parameter searches including association constants to determine the role of this parameter in predicting the reactivity of potential simulants towards NaOH, under the experimental conditions described.[†] All predictive models were determined using Equations 1 and 2, to allow for the determination of both two and three parameter combinations with a direct and inverse linear relationship. Five datasets were produced taking into account the limitations of the experiments conducted: (1) all data generated for all parameters and potential simulants listed in Figure 1 and Table 2; (2) exclusion of association constant (P_1) from the complete data set (1); (3) exclusion of simulant data for those compounds, which exhibit association constant values less than $10 M^{-1}$ from the P_1 data set, as these values are known to fall outside of experimental limitations; (4) exclusion of percentage breakdown data from P_0 , where potential simulant breakdown was found to be $<10\%$ over 6 hours, as these values were thought to fall outside of experimental

Table 2. List of parameters (P) used to produce potential simulant predictive models. $P_1 - P_{20}$ are previously published data sets[11]. The experimental methods used to calculate $P_0 - P_{20}$ are detailed within the supplementary information.†

Parameter number	Parameter	Parameter description
P_0	Breakdown after 6 hours (%)	Percentage breakdown after 6 hours determined via ^1H NMR experiments.
P_1	Association constant (M^{-1})	Association constant derived using a 1:1 binding isotherm.
P_2	E_{min} ($\text{kJ}\cdot\text{mol}^{-1}$)	Electrostatic surface energy minimum.
P_3	E_{max} ($\text{kJ}\cdot\text{mol}^{-1}$)	Electrostatic surface energy maximum.
P_4	Molecular Volume (\AA^3)	Total volume the molecule occupies.
P_5	Molecular Area (\AA^2)	Total molecular surface area.
P_6	Solvent accessible area (\AA^2)	Molecular surface area accessible with a 1.4 \AA radius probe.
P_7	Polar surface area (\AA^2)	Molecular surface area of any nitrogen and oxygen and any attached hydrogens.
P_8	% Polar surface area (\AA^2)	Percentage polar surface area.
P_9	Polarisability	How easily an electron cloud is distorted by an electric field.
P_{10}	Steric weighting factor (SWF) (\AA^2)	Molecular surface area within $1/8^{\text{th}}$ of the E_{min} .
P_{11}	Steric accessibility factor (SAF) (\AA^2)	Molecular surface area within $1/8^{\text{th}}$ of the E_{max} .
P_{12}	HOMO (eV)	Energy of the highest occupied molecular orbital.
P_{13}	LUMO (eV)	Energy of the lowest unoccupied molecular orbital.
P_{14}	Energy (kJ)	Total energy.
P_{15}	Electrostatic charge	The electrostatic charge of the HBA oxygen atom of the simulant.
P_{16}	Additive N \cdots O hydrogen bond length (\AA)	The sum of the N \cdots O hydrogen bond lengths calculated for a hydrogen bonded 1:1 complex of an appropriate simulant and non-specific hydrogen bond donating receptor 23 .
P_{17}	Log P	Calculated octanol water partition coefficient.
P_{18}	Dipole moment (D)	Separation of charge across the molecule.
P_{19}	Additive N-H \cdots O hydrogen bond length	The sum of the N-H \cdots O hydrogen bond lengths calculated for a hydrogen bonded 1:1 complex of an appropriate simulant and non-specific hydrogen bond donating receptor 23 .
P_{20}	Additive hydrogen bond angle difference from 180°	Sum of the N-H \cdots O angles difference from 180° , calculated for a hydrogen bonded 1:1 complex of an appropriate simulant and non-specific hydrogen bond donating receptor 23 .

limitations due to inherent integration errors; (5) and the exclusion of both association constant (P_1) < 10 M^{-1} and percentage breakdown values (P_0) < 10%.

$$P_0 = P_x^a \times P_y^b \quad (1)$$

$$|a| + |b| = 2$$

$$P_0 = P_x^a \times P_y^b \times P_z^c \quad (2)$$

$$|a| + |b| + |c| = 3$$

This approach allowed us to ascertain the importance of an experimental association constant, generated from a non-specific host:guest binding study, in the prediction of simulant reactivity. The models produced using these exhaustive search methods for datasets 1–5 were then ranked according to how well they fit the data in terms of their R^2 values. From this ranking, we then selected the 10 best fitting models for Equation 1 and Equation 2. This resulted in the production of 20 models of best fit for each dataset 1–5, giving 100 models in total. From this list, we then extracted the parameters that feature in these models and took those as being the most relevant ones for the prediction of the simulant properties. A summary of these data is shown in Figure 2.

Comparing all five data sets, parameters $P_2, P_3, P_4, P_7, P_8, P_9, P_{10}, P_{11}, P_{14}, P_{16}, P_{17}, P_{18}, P_{19}$ and P_{20} (see Table 2) occur ≤ 10 times within the 100 models. It is therefore unlikely that these parameters are significant for the construction of a predictive OP simulant breakdown model. These 100 models also indicate that P_{13} (LUMO Energy) should be considered a significant parameter with a total of 64

Table 3. Further physicochemical parameters calculated for 1–22. For experimental details see ESI.† Storage stability was monitored over a one-month period, samples were stored in sealed containers at room temperature, and the % breakdown then recorded. The hydrolytic stability of these potential simulants was ascertained in a DMSO:H₂O (70:30) solution, over 14 hr at 291 K, values reported represent % compound breakdown over this time frame. For liquid samples, the density, surface tension, and viscosity values were calculated at 298 K.

No.	Stability		Density (g·cm ⁻³)	Surface tension (mN·m ⁻¹)	Viscosity (mPa)
	Storage breakdown (%)	Hydrolytic breakdown (%)			
1	0	0	1.39	18.0	4.8
2	0	0	1.17	23.2	6.2
3	0	0	1.83	26.1	15.5
4	0	0	1.30	25.9	4.1
5	0	0	1.06	27.2	5.5
6	0	0	1.19	24.4	0.8
12	0	0	<i>a</i>	<i>a</i>	<i>a</i>
13	0	0	<i>a</i>	<i>a</i>	<i>a</i>
14	0	0	<i>a</i>	<i>a</i>	<i>a</i>
15	2	0	<i>a</i>	<i>a</i>	<i>a</i>
16	0	0	1.31	28.6	6.8
17	0	0	<i>a</i>	<i>a</i>	<i>a</i>
18	0	0	<i>a</i>	<i>a</i>	<i>a</i>
19	0	0	<i>a</i>	<i>a</i>	<i>a</i>
20	0	0	<i>a</i>	<i>a</i>	<i>a</i>
21	0	0	1.45	32.0	2.8
22	0	0	1.12	22.7	12.2

a = not a liquid under experimental conditions.

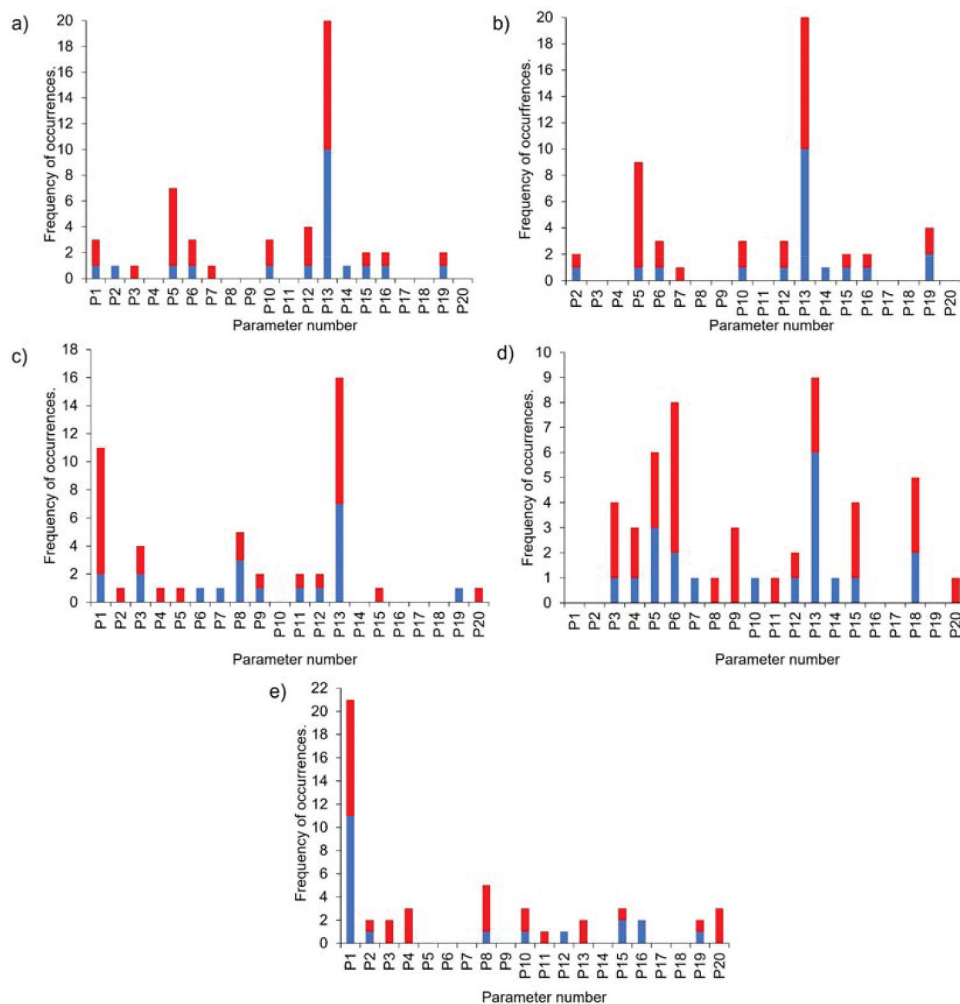


Figure 2. The frequency of occurrences in the top 10 models, produced by an exhaustive search of fits, ranked by R^2 analysis for each parameter to: i) Equation (1) (blue); and ii) Equation (2) (red), in a) dataset 1 (includes 440 data points in total), b) dataset 2 (includes 418 data points in total), c) dataset 3 (includes 240 data points in total), d) dataset 4 (includes 260 data points in total) and e) dataset 5 (includes 140 data points in total).

occurrences overall; this is not surprising as this orbital is directly involved in the reaction process. Gratifyingly, the parameter with the second highest number of occurrences is P_1 (the association constant), with a total of 35 occurrences over the 80 models, where this parameter was included within the initial datasets (Figure 2(a,c,d,e)). Furthermore, the occurrences of this parameter were limited to models that were produced by data sets 3 and 5 (Figure 2(c,e)). Importantly, it is these two datasets that consider the experimental limitations of association constant determination – in effect, the good fit arises after excluding the noise. In addition, as highlighted in Figure 2(d), where the experimental limitations are considered for the % simulant breakdown, but not for the association constant parameters, we see the occurrence of P_1 drop to

zero, supporting the importance of including such limitations in these datasets. After screening, the 20 models with the highest R^2 values used data set 5 (Figure 2(e)) which takes into account the experimental limitations placed on both the reactivity and association constant data. Within these models, the association constant parameter (P_1) occurs 21 times. We therefore believe that this result confirms that experimental association constants for hydrogen bonded complex formation can be utilised in the construction of predictive reactivity models for the identification of OP simulants.

When comparing the top 20 models, defined by R^2 analysis, through the fitting of datasets 1–5 to Equations (1) and (2), the models produced from dataset 5 reported the highest R^2 values. Of these top 20 predictive models, those produced using

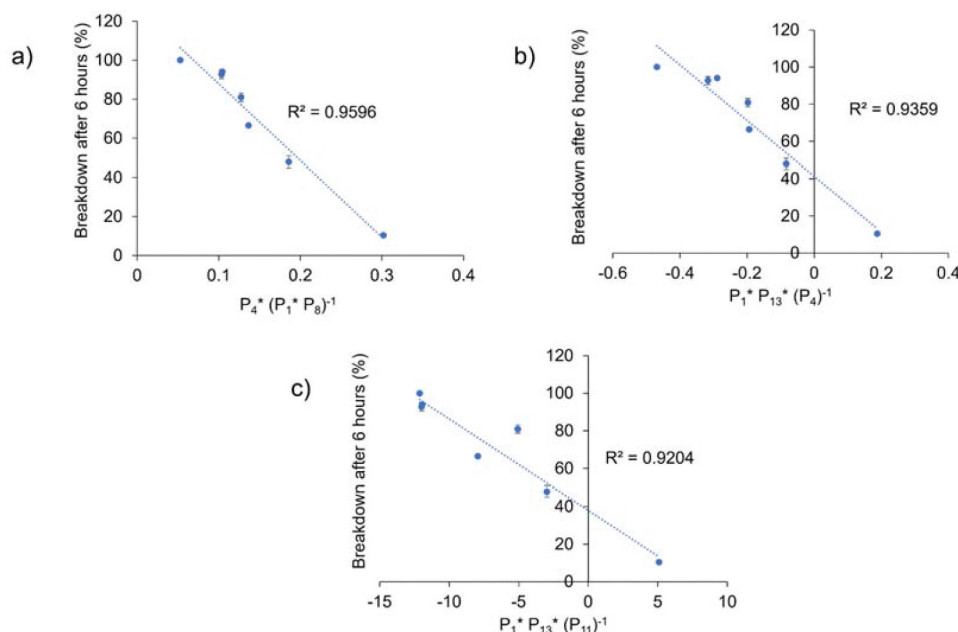


Figure 3. Top three predictive simulant breakdown models defined through the ranking of R^2 values (from highest to lowest), obtained from fitting datasets 1–5 to Equations (1) and (2). The models shown in a–c were generated from dataset 5.

Equation (2) reported higher R^2 values than from Equation (1). The models reporting the three highest R^2 values ($R^2 = 0.9596$, 0.9359 and 0.9204 respectively) have been identified as current lead predictive models and are shown in Figure 3. These models include i) Figure 3(a) – P_1 (association constant), P_4 (molecular volume) and P_8 (% polar surface area); ii) Figure 3(b) – P_1 (association constant), P_4 (molecular volume) and P_{13} (LUMO); iii) Figure 3(c) – P_1 (association constant), P_{11} (SAF) and P_{13} (LUMO).

Physical property considerations

In addition to breakdown rate, there may be other physical properties required of a simulant to make its use practical in exercises such as live testing scenarios. The choice of simulant is therefore often a compromise between competing demands, for example the simulant might have to be readily available in advance of live experiment and thus require medium/long-term storage. Considering possible practical requirements, we explored several physical parameters for the simulants detailed herein: storage stability, viscosity, hydrolytic stability, density, and surface tension. The key values are summarised in Table 3; the remainder can be found within the ESI.[†]

Conclusion

We have identified three predictive models for potential OP CWA simulant breakdown in the presence of five equivalents of NaOH, in a methanol- d_4 :D₂O 70:30 solution at 291 K. It is envisioned that the development of such predictive methodologies will enable the production of next-generation OP CWA decontamination technologies that rely on nucleophilic breakdown reaction mechanisms specifically. Additionally, we have shown the importance of considering experimental limitations on both association constant and reactivity datasets. The breakdown data are supported by a variety of physicochemical characterisation data, which are of use selecting an appropriate OP CWA simulant. It is hoped that the use of structure activity relationships, achieved using similar, predictive methodologies to those detailed here, will enable the increasingly effective identification of appropriate simulants to aid in combatting the threat of OP CWAs.

Acknowledgments

R. Ellaby, D. Chu, A. Pepes, E. R. Clark and J. Hiscock would like to thank the University of Kent for funding. Additionally, J. Hiscock would also like to thank UKRI for the funding of her Future Leaders Fellowship (MR/T020415/1).

Disclosure statement

No potential conflict of interest was reported by the author(s).

Funding

This work was supported by the UK Research and Innovation [MR/T020415/1].

Supplementary material

Supplemental data for this article can be accessed here.

References

- [1] Delfino RT, Ribeiro TS, Figueroa-Villar JD. Organophosphorus Compounds as Chemical Warfare Agents: a Review. *J Braz Chem Soc.* **2009**;20(3):407–428.
- [2] Badr AM. Organophosphate toxicity: updates of malathion potential toxic effects in mammals and potential treatments. *Environ Sci Pollut Res.* **2020** July 1;27(21):26036–26057. Springer.
- [3] Aroniadou-Anderjaska V, Aplan JP, Figueiredo TH, et al. Acetylcholinesterase inhibitors (Nerve agents) as weapons of mass destruction: history, mechanisms of action, and medical countermeasures. *Neuropharmacology.* **2020** December 15;181:108298. Elsevier Ltd.
- [4] Statement by the Federal Government on the Navalny case. [Cited 2021 May 24. <https://archiv.bundestag.de/archiv-de/meta/startseite/state-statement-by-the-federal-government-on-the-navalny-case-1781882>
- [5] Peplow M. Nerve Agent Attack Used 'Novichok' Poison. *C&EN Glob. Enterp.* **2018**;96(12):3
- [6] Nakagawa T, Tu AT. Murders with VX: Aum Shinrikyo in Japan and the assassination of Kim Jong-Nam in Malaysia. *Forensic Toxicology.* **2018** July 1;36(2):542–544. Springer Tokyo.
- [7] John H, van der Schans MJ, Koller M, et al. Fatal Sarin poisoning in Syria 2013: forensic verification within an international laboratory network. *Forensic Toxicol.* **2018**;36(1):61–71.
- [8] Okumura T, Takasu N, Ishimatsu S, et al. Report on 640 victims of the Tokyo subway Sarin attack. *Ann Emerg Med.* **1996**;28(2):129–135.
- [9] Kirlikovali KO, Chen Z, Islamoglu T, et al. Zirconium-based metal-organic frameworks for the catalytic hydrolysis of organophosphorus nerve agents. *ACS Appl Mater Interfaces.* **2020**;12(13):14702–14720.
- [10] Emelianova A, Basharova EA, Kolesnikov AL, et al. Force fields for molecular modeling of Sarin and its simulants: DMMP and DIMP. *J Phys Chem B.* **2021**;125(16):4086–4098.
- [11] Ellaby RJ, Clark ER, Allen N, et al. Identification of organophosphorus simulants for the development of next-generation detection technologies. *Org Biomol Chem.* **2021**;19(9):2008–2014.
- [12] Bartelt-Hunt SL, Knappe DRU, Barlaz MA. A review of chemical warfare agent simulants for the study of environmental behavior. *Crit Rev Environ Sci Technol.* **2008**;38(2):112–136.
- [13] Sambrook MR, Vincent JC, Ede JA, et al. Experimental and computational study of the inclusion complexes of β -cyclodextrin with the chemical warfare agent Soman (GD) and commonly used simulants. *RSC Adv.* **2017**;7(60):38069–38076.
- [14] Sambrook MR, Gass IA, Cragg PJ. Spectroscopic and inclusion properties of G-series chemical warfare agents and their simulants: a DFT study. *Supramol Chem.* **2018**;30(3):206–217.
- [15] Ede JA, Cragg PJ, Sambrook MR. Comparison of binding affinities of water-soluble calixarenes with the organophosphorus nerve agent Soman (GD) and commonly-used nerve agent simulants. *Molecules.* **2018**;23(1):207.
- [16] Williams GT, Haynes CJE, Fares M, et al. Advances in applied supramolecular technologies. *Chem Soc Rev.* **2021**;50(4):2737–2763.
- [17] Sambrook MR, Notman S. Supramolecular chemistry and chemical warfare agents: from fundamentals of recognition to catalysis and sensing. *Chem Soc Rev.* **2013**;42(24):9251–9267.
- [18] Hiscock JR, Sambrook MR, Cranwell PB, et al. Tripodal molecules for the promotion of phosphoester hydrolysis. *Chem Commun.* **2014**;50(47):6217–6220.
- [19] Hiscock JR, Sambrook MR, Ede JA, et al. Disruption of a binary organogel by the chemical warfare agent Soman (GD) and common organophosphorus simulants. *J Mater Chem A.* **2015**;3(3):1230–1234.
- [20] Hiscock JR, Kirby IL, Herniman J, et al. Supramolecular gels for the remediation of reactive organophosphorus compounds. *RSC Adv.* **2014**;4(85):45517–45521.
- [21] Hiscock JR, Sambrook MR, Wells NJ, et al. Detection and remediation of organophosphorus compounds by oximate containing organogels. *Chem Sci.* **2015**;6(10):5680–5684.
- [22] Taylor CGP, Piper JR, Ward MD. Binding of chemical warfare agent simulants as guests in a coordination cage: contributions to binding and a fluorescence-based response. *Chem Commun.* **2016**;52(37):6225–6228.
- [23] Taylor CGP, Metherell AJ, Argent SP, et al. Coordination-cage-catalysed hydrolysis of organophosphates: cavity- or surface-based? *Chem - A Eur J.* **2020**;26(14):3065–3073.
- [24] Sambrook MR, Althoff MA, Karaghiosoff KL, et al. Coordination behavior of organothiophosphate ligands towards trivalent lanthanide complexes and potential use as V-series chemical warfare agent simulants. *J Coord Chem.* **2019**;72(12):2115–2126.
- [25] Ruffley JP, Goodenough I, Luo TY, et al. Design, synthesis, and characterization of metal-organic frameworks for enhanced sorption of chemical warfare agent simulants. *J Phys Chem C.* **2019**;123(32):19748–19758.
- [26] Lavoie J, Srinivasan S, Nagarajan R. Using cheminformatics to find simulants for chemical warfare agents. *J Hazard Mater.* **2011**;194:85–91.

- [27] Mendonca ML, Snurr RQ. Screening for improved nerve agent simulants and insights into organophosphate hydrolysis reactions from DFT and QSAR modeling. *Chemistry*. **2019**;25(39):9217–9229.
- [28] Mendonca ML, Snurr RQ. Screening for improved nerve agent simulants and insights into organophosphate hydrolysis reactions from DFT and QSAR modeling. *Chem A Eur J*. **2019**;25(39):9118.
- [29] White LJ, Wells NJ, Blackholly LR, et al. Towards quantifying the role of hydrogen bonding within amphiphile self-association and resultant aggregate formation. *Chem Sci*. **2017**;8(11):7620–7630.
- [30] Tyuleva SN, Allen N, White LJ, et al. Approach to the design of novel amphiphiles with antibacterial properties against MSRA. *Chem Commun*. **2019**;55(1):95–98.
- [31] Allen N, White LJ, Boles JE, et al. Towards the prediction of antimicrobial efficacy for hydrogen bonded, self-associating amphiphiles. *ChemMedChem*. **2020**;15(22):2193–2205.
- [32] Beer S, Prasad GK, Pandey KS, et al. Decontamination of chemical warfare agents. *Def. Sci. J*. **2010**;60(4):428–441
- [33] Altmann H-J, Richardt A Decontamination of chemical warfare agents. *Decontam. Warf. Agents Enzym. Methods Remov. B/C Weapons*. **2008**, 83–115.
- [34] Panmand DS, Tiwari AD, Panda SS, et al. New benzotriazole-based reagents for the phosphorylation of various N-, O-, and S-Nucleophiles. *Tetrahedron Lett*. **2014**;55(43):5898–5901.
- [35] Huang H, Ash J, Kang JY. Tf₂O-Promoted activating strategy of phosphate analogues: synthesis of mixed phosphates and phosphinate. *Org Lett*. **2018**;20(16):4938–4941.
- [36] Feng S, Li J, Wei J. Ionic liquid brush as an efficient and reusable heterogeneous catalytic assembly for the tosylation of phenols and alcohols in neat water. *New J Chem*. **2017**;41(12):4743–4746.
- [37] Schoonover DV, Gibson HW. Facile removal of tosyl chloride from tosylates using cellulosic materials, e.g., filter paper. *Tetrahedron Lett*. **2017**;58(3):242–244.
- [38] Chang JWW, Chia EY, Chai CLL, et al. Scope of direct arylation of fluorinated aromatics with Aryl Sulfonates. *Org Biomol Chem*. **2012**;10(11):2289–2299.
- [39] Noji T, Fujiwara H, Okano K, et al. Synthesis of substituted indoline and Carbazole by Benzyne-Mediated cyclization-functionalization. *Org Lett*. **2013**;15(8):1946–1949.
- [40] Ortega N, Feher-Voelger A, Brovotto M, et al. Iron(III)-Catalyzed halogenations by substitution of sulfonate esters. *Adv Synth Catal*. **2011**;353(6):963–972.
- [41] Busschaert N, Kirby IL, Young S, et al. Squaramides as potent transmembrane anion transporters. *Angew Chemie Int Ed*. **2012**;51(18):4426–4430.
- [42] Chen YF, Kao CL, Lee WK, et al. ¹³C-Isotope labeled surrogate for estimating organophosphorus pesticides in agricultural products by gas chromatography-mass spectrometry. *J Chin Chem Soc*. **2016**;63(9):751–757.
- [43] Ma W, Mt K, Bm H, et al. Strategies to protect the health of deployed U.S. Forces: Force Protection and Decontamination, **1999**.
- [44] Romano J Jr, Salem A, Lukey H, et al. Chemical warfare agents: chemistry, pharmacology, toxicology, and therapeutics. 2nd ed. CRC Press: USA; **2007**.
- [45] Jang YJ, Kim K, Tsay OG, et al. Destruction and detection of chemical warfare agents. *Chem Rev*. **2015**;115(24):5345–5403.
- [46] Farquharson S, Inscore FE, Christesen S. Detecting chemical agents and their hydrolysis products in water. *Top Appl Phys*. **2006**;103:447–461.
- [47] Wilson C, Cooper NJ, Briggs ME, et al. Investigating the breakdown of the nerve agent simulant Methyl Paraoxon and chemical warfare agents GB and VX using nitrogen containing bases. *Org Biomol Chem*. **2018**;16(47):9285–9291.
- [48] R: The R project for statistical computing. [cited 2021 May 24] <https://www.r-project.org>
- [49] Doyle AG, Jacobsen EN. Small-Molecule H-Bond donors in asymmetric catalysis. *Chem Rev*. **2007**;107(12):5713–5743.
- [50] Madarász Á, Dósa Z, Varga S, et al. Thiourea derivatives as brønsted acid organocatalysts. *ACS Catal*. **2016**;6(7):4379–4387.
- [51] Serdyuk OV, Heckel CM, Tsogoeva SB. Bifunctional primary Amine-Thioureas in asymmetric organocatalysis. *Organic and Biomolecular Chemistry*. **2013**;11(41):7051–7071
- [52] de Villegas D, Gálvez MD, Etayo JA, et al. Advances in enantioselective organocatalyzed anhydride desymmetrization and its application to the synthesis of valuable enantiopure compounds. *Chem Soc Rev*. **2011**;40(11):5564–5587.
- [53] Taylor MS, Jacobsen EN Asymmetric catalysis by Chiral Hydrogen-Bond donors. *Angewandte Chemie - International Edition*., **2006**, 1520–1543.